Molecular Intercalation in Black Phosphorus with Tunable Bandgaps for Infrared Photoelectric Materials

Feihong Chu,[a] Rongkun Zhou,[a] Beiyun Liu,[a] Wencai Zhou,[a] Hui Yan,[a] Zilong Zheng,*[a] and Yongzhe Zhang*[b]

[a] Key Laboratory of Advanced Functional Materials, Ministry of Education, Faculty of Materials and Manufacturing, Beijing University of Technology, Beijing, 100124, China.

[b] Key Laboratory of Optoelectronics Technology, Ministry of Education, Faculty of Information Technology, Beijing University of Technology, Beijing 100124, China.

Corresponding Author

*E-mail: zilong.zheng@bjut.edu.cn.

*E-mail: yzzhang@bjut.edu.cn.

Obtaining fraction of few-layer BP from molecular dynamics simulation

The BP atomic coordinates of the equilibrium structure were extracted from MD simulations. By calculating the distance between one BP layer and the neighbor BP layers, it can determine whether the BP layers were separated from the neighbor layers by CTAB molecules insertion. Considering the atomic vibrations, the distance (which judge whether the neighbor BP layers are separated or not) should be longer than interlayer distance (5.3 Å) of bulk BP. Therefore, when both two distances between the one BP layer and the two neighbor layers are longer than 7 Å (we assumed the change in bond length induced by vibration cannot be longer than 1.7 Å), the one BP layer was be considered as monolayer BP, as shown in Fig. S1a in SI. When the one distances shorter than 7 Å, the other one is longer than 7 Å, the configuration could be considered as few-layered BP. if the former sider do not have direct contact (d >7 Å) with another BP layer, we then can define it as the bilayer BP structure, see Fig. S1b. By employing the same algorithm, we could define trilayer, four-layer, five-layer as well.

Monolayer BP in hybrid superlattice

(a)

d > 7 Å

d > 7 Å

Bilayer BP in hybrid superlattice
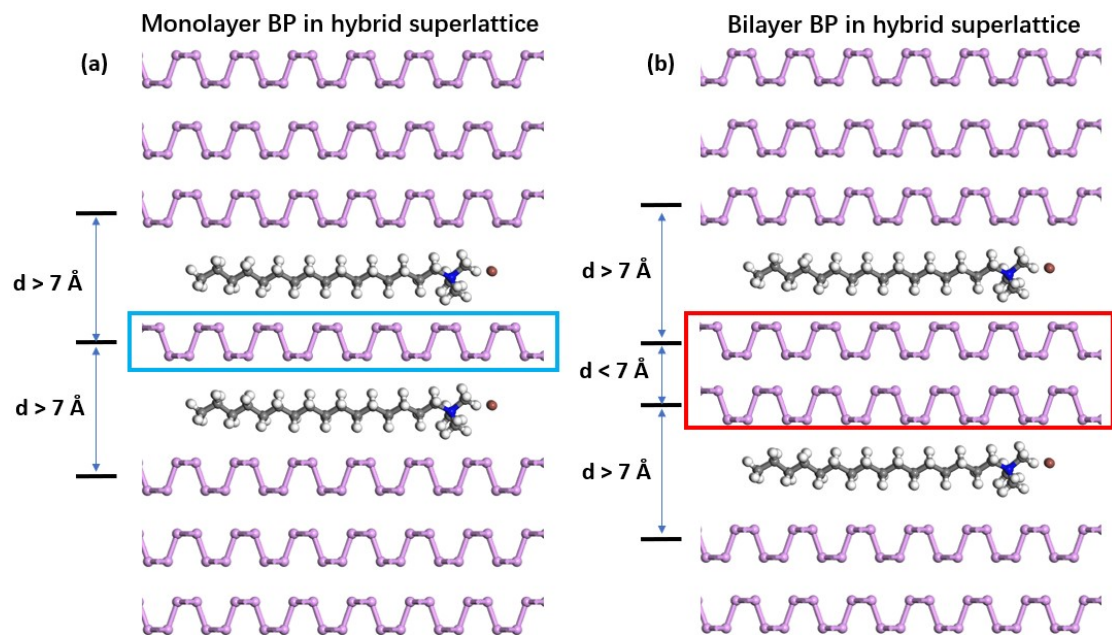
(b)

d > 7 Å

d < 7 Å

d > 7 Å

Fig. S1   Schematic structural views of (a) monolayer BP and (b) bilayer in hybrid superlattices, blue and red rectangles represent monolayer and bilayer BP, respectively.
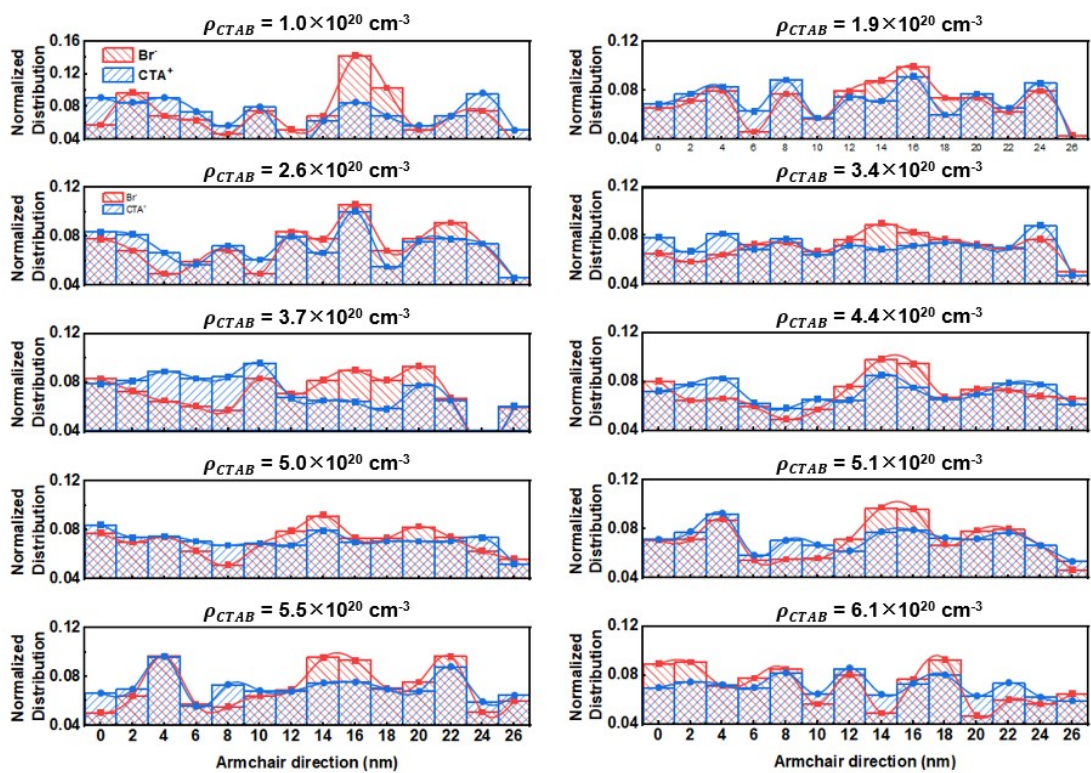
Fig. S2   Normalized distributions of Br⁻ and CTAB⁺ ions in hybrid superlattice.
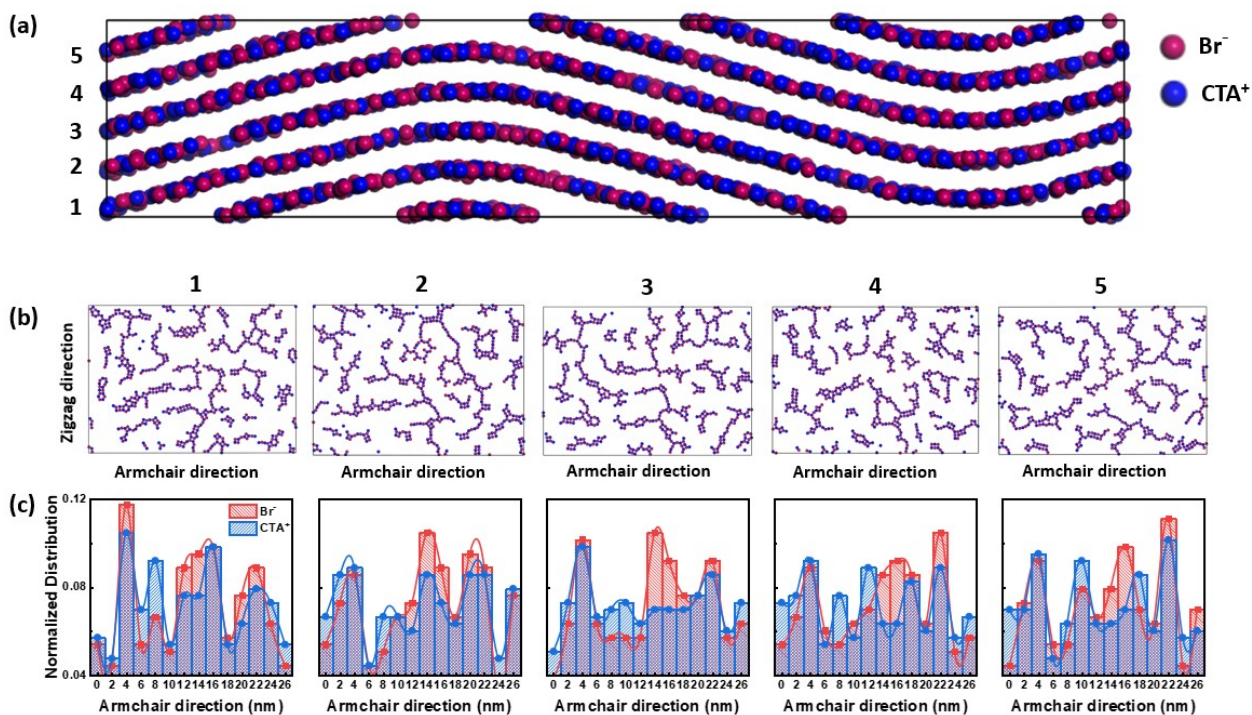
Fig. S3   (a) Position distributions of Br⁻ and CTAB⁺ ions in hybrid superlattice (ρ_{CTAB} = 5.5✗10²⁰ cm⁻³), (b) Position distributions of Br⁻ and CTAB⁺ ions in an individual CTAB molecular layer (The numbers correspond to Fig. S3a), in order to clearly observe the ion distribution, CTAB⁺ ion is simplified as blue ball, red ball represents Br⁻ ion, black phosphorus atoms are hidden. (c) Normalized distributions of Br⁻ and CTAB⁺ ions in an individual CTAB molecular layer (The numbers correspond to Fig. S3a).
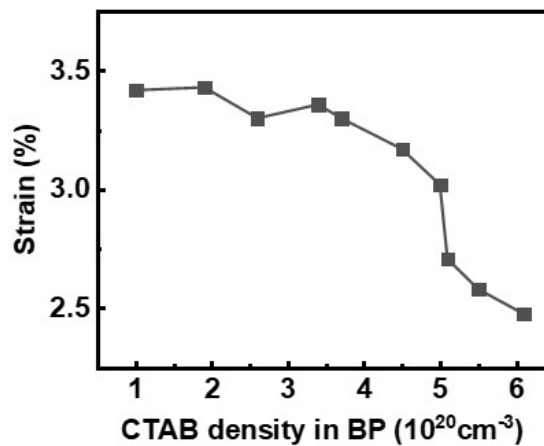
Fig. S4   Strain of hybrid superlattice in armchair direction as function of intercalated CTAB density.
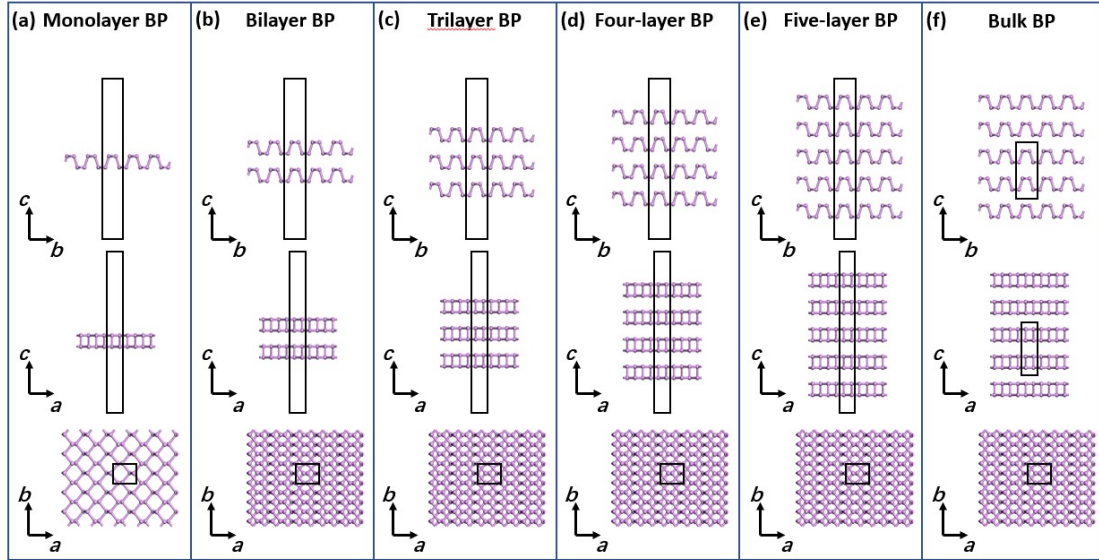
Fig. S5   Schematic structural views of few layer BP along the *a*, *b* and *c* directions, (a) monolayer, (b) bilayer, (c) trilayer, (d) four-layer, (e) five-layer and (f) bulk, respectively.

Table S1   Structural information for of optimized few-layer BP via DFT method.

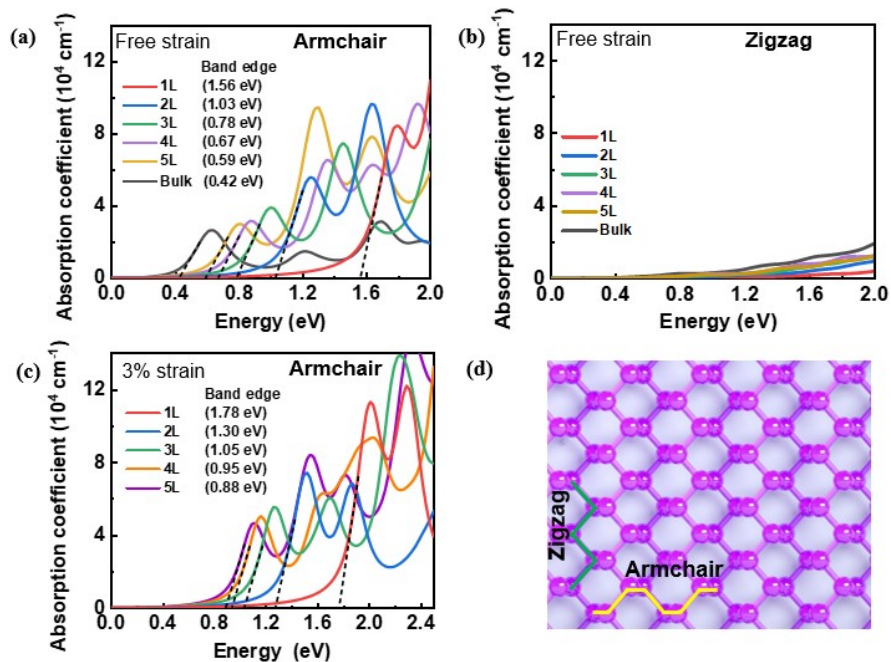| Layer number	*a* (Å)	*b* (Å)	*c* (Å)
1	3.31	4.57	
2	3.31	4.51	
3	3.32	4.48	
4	3.32	4.47	
5	3.32	4.46	
Bulk	3.32	4.44	5.28

Fig. S6   Estimated absorption coeffieients of few-layer BP with free strain (including monolayer, bilayer, trilayer, four-layer, five-layer, and bulk) along (a) armchair and (b) zigzag directions, respectively. (c) Estimated absorption coeffieient of few-layer BP with 3% strain along armchair directions. (d) Schematic armchair direction (yellow line) and zigzag direction (green line) on few-layer PB.
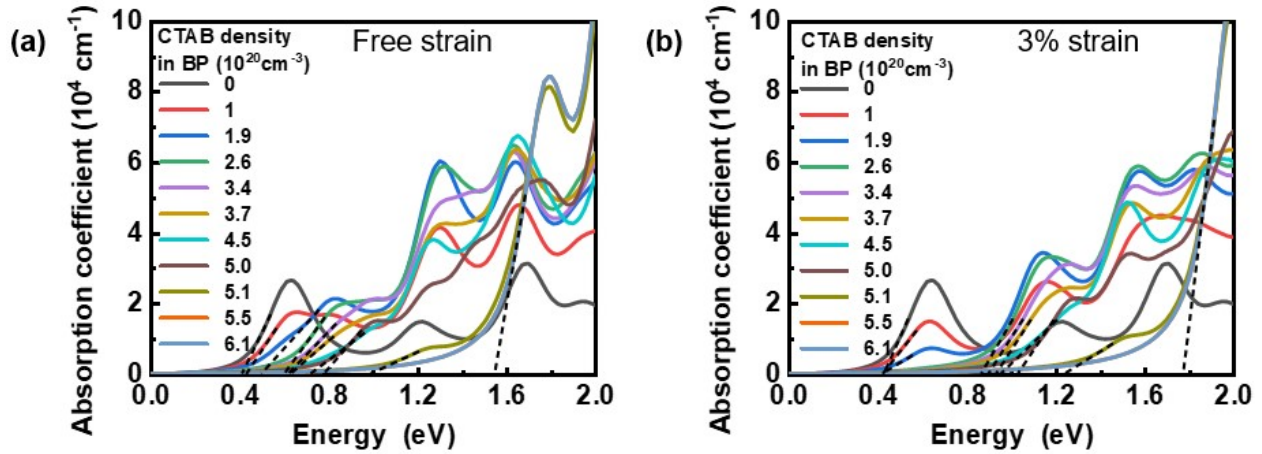
Fig. S7   Simulated absorptions coeffieient with different intercalated CTAB density (from 0 cm^{-3} up to 6.1⊘10^{20} cm^{-3}) in hybrid superlattice with (a) free strain and (b) 3% strain, the black dashed lines showed approximate linear fits in order to estimate the band edges.
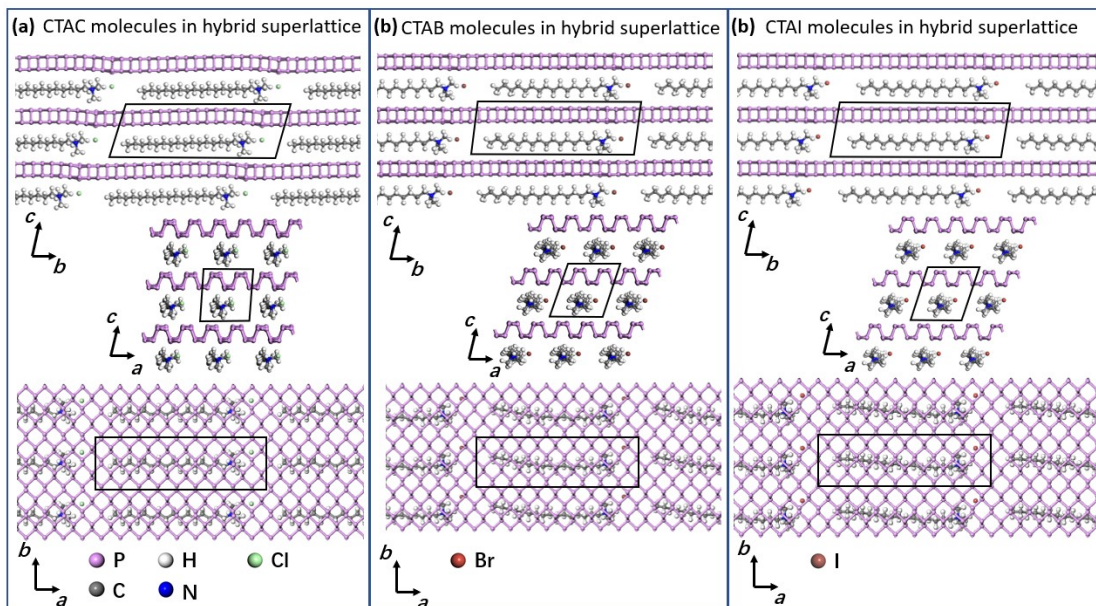
Fig. S8   Schematic structural views of hybrid superlattice with different interaction molecule, (a) CTAC, (b) CTAB and (c) CTAI, respectively.

Table S2   Structural information for hybrid superlattice obtained by DFT method.

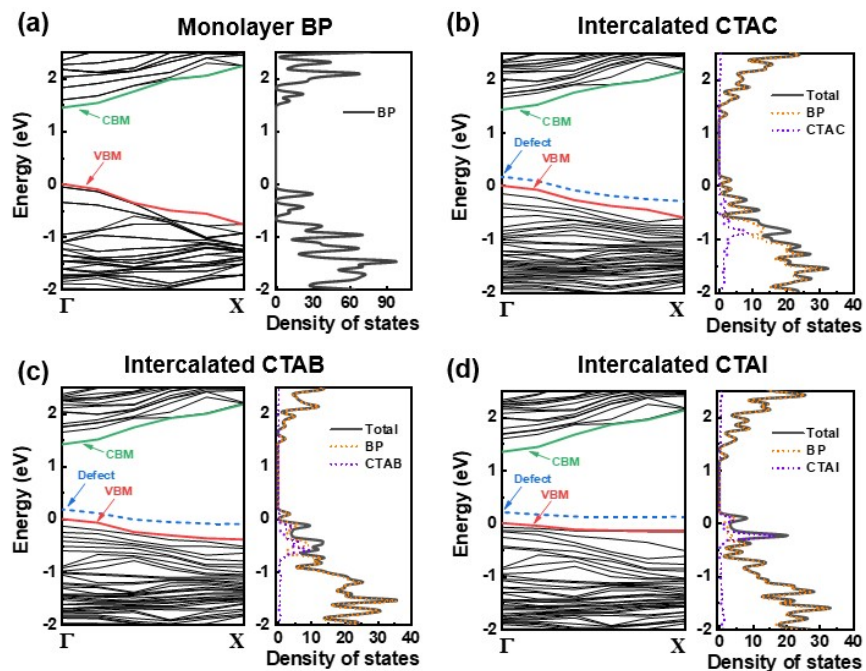| Intercalated molecule	a (Å)	b (Å)	c (Å)
CTAC	9.1	29.9	10.0
CTAB	9.1	29.9	10.5
CTAI	9.0	29.9	10.3

Fig. S9   Band structure and the density of states of monolayer BP and hybrid superlattices. (a) monolayer BP and the intercalated (b) CTAC molecules, (c) CTAB molecules, (d) CTAI molecules in hybrid superlattice. The red, green and blue solid line represent VBM band, CBM band, defect states, respectively. The purple and orange dashed line represent density of states of intercalated molecules and BP, respectively
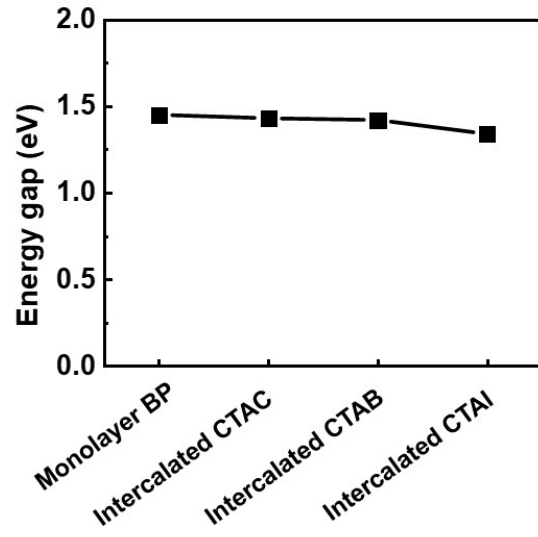
Fig. S10   Bandgaps of hybrid superlattices with intercalated CTAC, CTAB and CTAI molecules.

Superlattice absorption band edges with various intercalated molecules

Partial charge distributions of superlattices are obtained, as shown in Fig. S11. The charge distributions of VBM, CBM and defect states at Γ point are marked in red, green and blue, respectively. Absorption spectra of monolayer BP and hybrid superlattice with intercalated molecules is shown in Fig. S12. The absorption edges of hybrid superlattice are slightly different from monolayer BP. The intensity of the first absorption peak of hybrid superlattice are almost the same as each other. Since the electronic spatial distributions are separated away from each other between those defect states and CBM, and there are not any transition dipole moments between CBM and those defect states. The overlap between the charge distribution of the VBM and the CBM is significantly larger than the overlap between the charge distribution of the defect and the CBM.
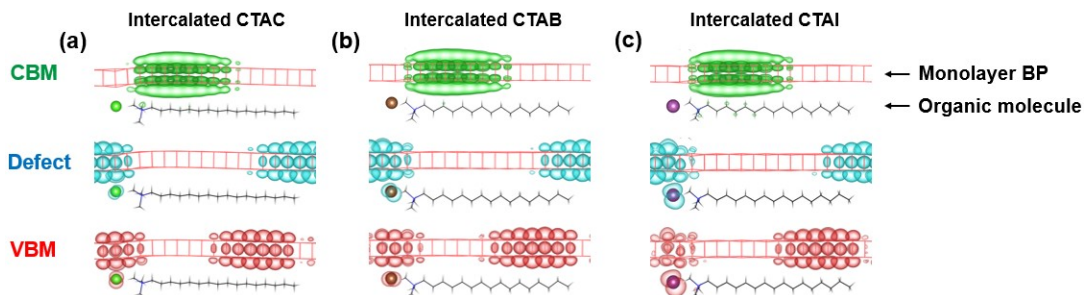

Fig. S11   Partial charge distributions of the intercalated CTAC molecules, CTAB molecules, CTAI molecules in hybrid superlattice. Charge distribution of VBM, CBM and defect states at Γ point are marked in red, green and blue, respectively.
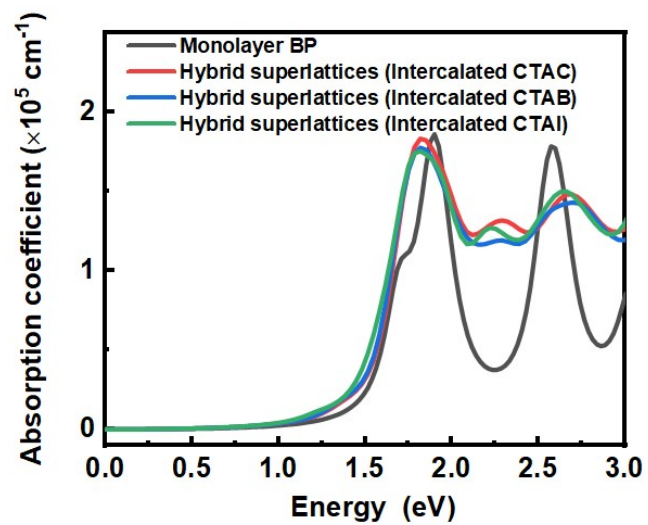
Fig. S12   Absorption coefficients of monolayer BP, and intercalated molecules in hybrid superlattices.